

Removal of heavy metal ions from aqueous solution using *Populus nigra* sawdust-based activated carbon

Syed Muhammad Salman^a, Fouzia Kamal^a, Muhammad Zahoor^{b,*}, Muhammad Wahab^a, Durre Shahwar^c, Hizb Ullah Khan^d, Syed Lal Badshah^a, Syed Nusrat Shah^e, Maria Sadia^b, Abdul Waheed Kamran^b

^aDepartment of Chemistry, Islamia College University Peshawar, 25000, KPK, Pakistan, emails: salman@icp.edu.pk (S.M. Salman), fouziakamal20@gmail.com (F. Kamal), mwahabbajaur@gmail.com (M. Wahab), shahbiochemist@gmail.com (S.L. Badshah)

^bDepartment of Biochemistry, University of Malakand, Chakdara Dir Lower, 18800, KPK, Pakistan, emails: mohammadzahoorus@yahoo.com (M. Zahoor), mariasadia@gmail.com (M. Sadia), waheedkamran1989@gmail.com (A.W. Kamran)

^cDepartment of Zoology, Islamia College University Peshawar, 25000, KPK, Pakistan, email: salmanchemist80@yahoo.com

^dDepartment of Chemistry, University of Science and Technology, Bannu, 28350, KPK, Pakistan, email: hizbmarvat@yahoo.com

^eDepartment of Chemistry, Bacha Khan University Charsadda, 24540, KPK, Pakistan, email: syednusratshah1@gmail.com

Received 13 August 2020; Accepted 21 January 2021

ABSTRACT

In this study, an activated carbon (AC) was prepared from *Populus nigra* sawdust and was used to remove Cd(II), Cr(VI) and Pb(II) ions from aqueous media. Instrumental techniques such as Fourier transform infrared spectroscopy, scanning electron microscopy, thermal gravimetric analysis, X-ray diffraction, energy dispersive X-ray and surface area analysis were used to characterize the prepared adsorbent. Batch adsorption experiments were conducted to enumerate the adsorption parameters and get optimum conditions for the effective adsorption of the selected heavy metals. The equilibrium data were evaluated through Freundlich, Langmuir, Temkin, Jovanovic and Harkins–Jura isotherm models. The Langmuir model best fitted the equilibrium data with high values of R^2 . Pseudo-first order, pseudo-second order, power function, intraparticle diffusion, and Natarajan–Khalaf models were used to evaluate the experimental kinetics data. Pseudo-second order model amongst them was found to be the best to fit the data well with high regression constant values of 0.9923, 0.9932 and 0.99112, respectively for Cr(VI), Cd(II) and Pb(II) sorption on AC. The thermodynamic parameters such as ΔH° , ΔS° and ΔG° were estimated for the sorption of selected heavy metals on AC, using Van't Hoff equation. From the estimated values of the mentioned parameters, it was inferred that the sorption of these metals on AC is favourable, spontaneous and exothermic in nature.

Keywords: *Populus nigra*; Sawdust; Adsorption; Isotherm; Thermo-dynamic parameters

1. Introduction

The heavy metal pollution is a major concern to the common and scientific communities around the world as they are deadly toxic and can accumulate in tissues and organs of both animals and plants. As human is on the

top of food chain thus their ultimate sink is human [1]. Wastewaters coming out from industries containing heavy metals adversely affect the environment and human health [1,2]. Due to their non-biodegradable nature these metals exist for long time in aqueous environment and in soil. Therefore, different approaches have been used to remove

* Corresponding author.

them from industrial effluents before reaching into water reservoirs [3]. Heavy metals such as Cd(II), Cr(VI) and Pb(II) are considered as the most toxic pollutants. Cadmium is released to aqueous media from many industries such as metal plating, smelting, pigments, mining, coating and the burning of fossil fuel and is responsible for itai-itai disease in humans, characterized by severe bone pain [4,5]. Cr(VI) is a powerful oxidant and its compounds are used in photography, as pigment in plastics, inks, paints and other dyes synthesis. Cr(VI) is used in steel production, tanning leather, preservation of wood, textile dyes and coating of corrosive materials. Cr(III) is less toxic and immobile while Cr(VI) is more toxic that can easily be absorbed by the skin due to its strong oxidizing ability and moves through soils to aquatic environment [6,7]. The main sources of lead pollution are mining, paints, pigment, electroplating, batteries manufacturing, and coal burning. It may cause anaemia, malaise, brain damage, loss of appetite, anorexia, kidney and liver diseases [6,7].

Many techniques such as ion exchange, electrolysis, flocculation, photo catalytic degradation, advanced oxidation, and membrane technologies are in use to remove heavy metals from aqueous media [8–16]. All of them have some drawbacks such as partial metal removal, high reagent cost and energy requirements, generation of large quantities of sludge and aggregation of metal precipitates while fouling in case of membranes. Phytoremediation is another technique that utilizes living plants for heavy metals removal from soil but it also has some disadvantages such as accumulation of pollutants in edible parts of the plant and are very slow, thus not practical [17]. Although some of these modern techniques are quite effective in removal of heavy metals from water, due to their expensive nature they are not used practically in every part of the world. Therefore, the most valid and practical approach that is used for metal ions removal from water is adsorption. Practically adsorption technique is used everywhere in reclamation of the aquatic environment due to its low cost, environmental friendly nature and utilization of naturally and abundantly available biomass in preparation of the adsorbents [17,18]. Regeneration of such biomass-based adsorbents is easy that is one of the essential aspects that controls the economy of water treatment processes [19]. Adsorbents prepared from biomass can be effectively regenerated by acids (such as HCl, H₂SO₄, HNO₃, HCOOH and CH₃COOH), alkalis (such as NaOH, NaHCO₃, Na₂CO₃, KOH and K₂CO₃), salts (such as NaCl, KCl, (NH₄)₂SO₄, CaCl₂·2H₂O, NH₄NO₃, KNO₃ and C₆H₅Na₃O₇·2H₂O), deionized water, chelating agents, and buffer solutions (such as bicarbonate and phosphate) [20]. All these are common laboratory reagents. Several studies have shown that HCl is more effective in the regeneration of loaded adsorbents when compared with other stripping agents such as HNO₃, H₂SO₄ and NaOH [21].

The current research study was conducted to remove toxic heavy metals such as Cd(II), Cr(VI) and Pb(II) from water through an activated carbon prepared from *Populus nigra* sawdust. The adsorbent was characterized by different instrumental techniques such as Fourier transform infrared (FTIR), scanning electron microscopy (SEM), energy dispersive X-ray (EDX), X-ray diffraction (XRD), and surface area analysis. To determine the optimal conditions for the selected

metals adsorption, the effect of initial metal concentration, contact time, pH, temperature and adsorbent dosage was investigated using batch experiments. Stability of a given adsorbent is an important parameter especially in situations where the same adsorbent is re-used in multiple adsorption cycles. Therefore, the reusability of adsorbent was also evaluated.

2. Materials and methods

All reagents HCl (AR 37%), NaOH (97%), CdCl₂ (99%), Pb(NO₃)₂ (99.99%) and K₂Cr₂O₇ (99.99%), were purchased from BDH (Germany), Fisher (UK) and Merck (Pakistan).

2.1. Preparation of activated carbon

Activated carbon (AC) was prepared from sawdust of locally available *Populus nigra* plant, collected from District Malakand, KPK, Pakistan. About 100 g of sawdust was charred in an electric furnace containing an inlet for N₂ and outlet for various gases. The furnace temperature was initially raised to 400°C with a rate of 10°C/min and allowed to carbonize the material for about 1 h under an inert atmosphere of nitrogen. The temperature was further increased to the desired level of activation temperature, that is, 800°C at which the steam was introduced along with N₂ using a syringe pump. After keeping the process isothermal for 1 h, the furnace was switched off. When the room temperature was reached, the sample was taken out. In order to remove any ash present in the resultant mass, it was washed with 0.05 M HCl and then with distilled water. After washing, the residual mass was dried in an oven at 105°C for 6 h.

2.2. Preparation of heavy metal solutions

Stock solutions (1,000 ppm) of Cd(II), Cr(VI) and Pb(II) were prepared by dissolving 2.031 g of CdCl₂·H₂O, 2.837 g of K₂Cr₂O₇ and 1.599 g of Pb(NO₃)₂ in double distilled water. Working solutions of different concentration (20–200 ppm) were prepared using dilution formula.

2.3. Characterization of prepared adsorbent

The FTIR spectrophotometer (PerkinElmer, Merlin model 2000) was used to determine the functionalities in AC. Pellets were prepared by adding 0.3 g of KBr and 0.003 g of AC and pressed by applying 3–7 bar pressure. The surface morphology was visualized by scanning electron microscope (JEOL Japan-JSM 5910) at a voltage of 10 kV. The thermo-gravimetric analysis (TGA) was performed with diamond series (PerkinElmer, United States) analyser using alumina as a standard. To identify the nature of AC, the XRD (JDX-3532 JEOL, Japan) analysis was performed. Monochromatic radiation of nickel filter CuK α with wavelength 1.5418 was used at room temperature. Energy dispersive X-ray analysis (INCA200/Oxford Instruments, UK) was also carried out to determine elemental composition of the prepared adsorbent. Surface area of the adsorbent along with pore volume and diameter was determined using Quantachrome surface area analyser (NOVA, 2200e, United States).

2.4. Batch adsorption experiments

About 40 mL heavy metal solutions (20–200 mg L⁻¹) were contacted with 0.07 g of AC while the shaking speed was 160 rpm. The solution was filtered after shaking and in filtrates the remaining metal concentrations were determined by atomic absorption spectrophotometer (PerkinElmer USA-700 AAS). The amount of Cd(II), Cr(VI) and Pb(II) adsorbed, q_e (mg g⁻¹) and percentage removal (%R) were calculated using the following equations [22,23].

$$q_e = (C_i - C_f) \times \frac{V}{m} \quad (1)$$

$$\%R = \frac{(C_i - C_f)}{C_i} \times 100 \quad (2)$$

where C_i and C_f are the initial and final equilibrium metals concentration of Cd(II), Cr(VI) and Pb(II), V volume of solution (L) and m is the mass of AC.

Freundlich, Langmuir, Temkin, Jovanovic and Harkins–Jura models were utilized to analyse the adsorption equilibrium data.

2.5. Adsorption kinetic studies

To determine the kinetic parameters of metal ions adsorption on AC, 0.07 g of adsorbent was mixed with 40 mL of Cd(II), Cr(VI) and Pb(II) (100, 80 and 120 mg L⁻¹, respectively) metal solutions and shaken on a shaker at a speed of 160 rpm for 180 min. Pseudo-first and second order, power function, intraparticle diffusion and Natarajan–Khalaf models were applied to analyse the kinetic data.

2.6. Effect of solution pH and adsorbent dosage

To adjust pH of solution, NaOH solution (0.1 M) was prepared by dissolving 2 g NaOH in 500 mL distilled water while HCl solution (0.1 M) was prepared by adding

4.144 mL HCl (37%) into 500 mL of distilled water. Different pH solutions containing 100, 80 and 120 mg L⁻¹ of Cd(II), Cr(VI) and Pb(II), respectively were contacted with 0.07 g of AC and shaken for 180 min at 160 rpm. The remaining Cd(II), Cr(VI) and Pb(II) concentration after adsorption was determined through atomic absorption spectrophotometer. The effect of adsorbent dosage on Cd(II), Cr(VI) and Pb(II) adsorption was studied in range 0.01–0.1 g while other parameters were same as mentioned above.

2.7. Thermodynamic studies

The effect of temperature on Cd(II), Cr(VI) and Pb(II) adsorption on AC was studied at 25°C, 35°C, 45°C and 55°C keeping other parameters constant. Van't Hoff equation was applied to determine the values of thermodynamics parameters such as ΔH° , ΔS° and ΔG° .

3. Results and discussion

3.1. Characterization of AC

The FTIR spectrum of unloaded and loaded AC is shown in Figs. 2a–d. The peak at 3,450 to 3,280 cm⁻¹ indicates O–H group [24]. The peak between 1,500 and 1,600 cm⁻¹ indicates C=C stretching [25]. Peak at 2,926–2,854 cm⁻¹ shows C–H stretching [26]. Similarly, the peak at 1,212.53 cm⁻¹ shows the C–O group [27]. Peak at 755.10 presents the =C–H bending. The slight shifting of the peaks in loaded adsorbent confirms the adsorption of Cd(II), Cr(VI) and Pb(II) on prepared AC.

The SEM images are shown in Fig. 2e. The SEM image shows the morphology of adsorbent having irregular particle shape with shattered edges and crooks suggesting that the adsorbent has a suitable surface for heavy metals adsorption.

The TGA of AC is shown in Fig. 2f. The mass of sorbent analysed was 5.663 g. From 0°C to 60°C, the observed mass loss was 3%, which was due to water evaporation. The second mass loss was observed up to 380°C, which was due to

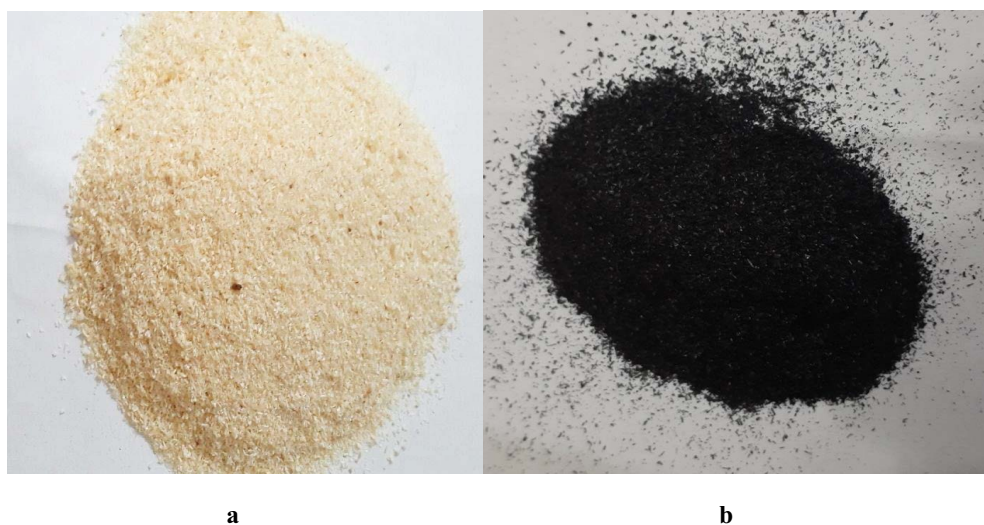


Fig. 1. (a) Sawdust of *Populus nigra* stem and (b) activated carbon prepared from sawdust.

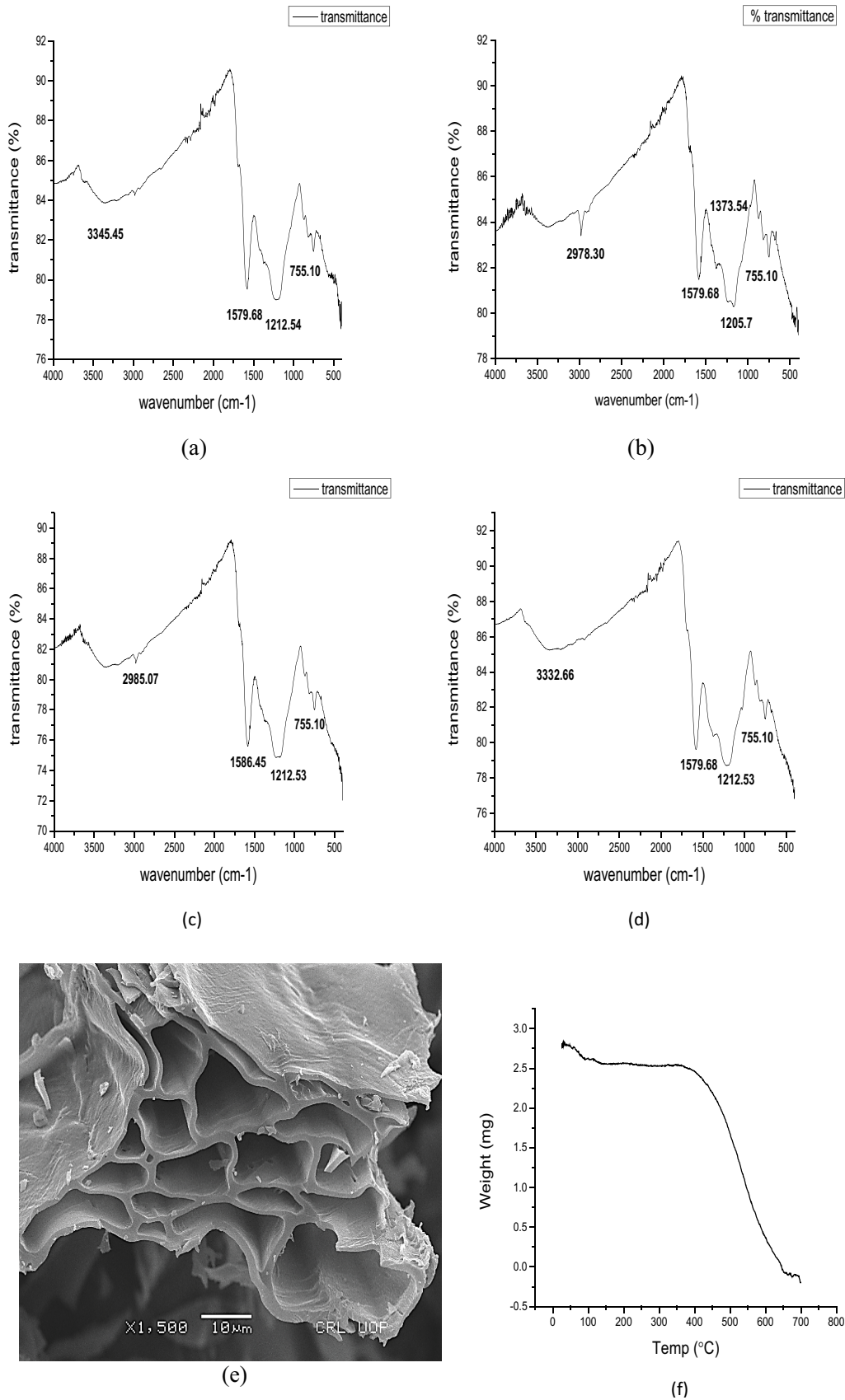


Fig. 2. Continued

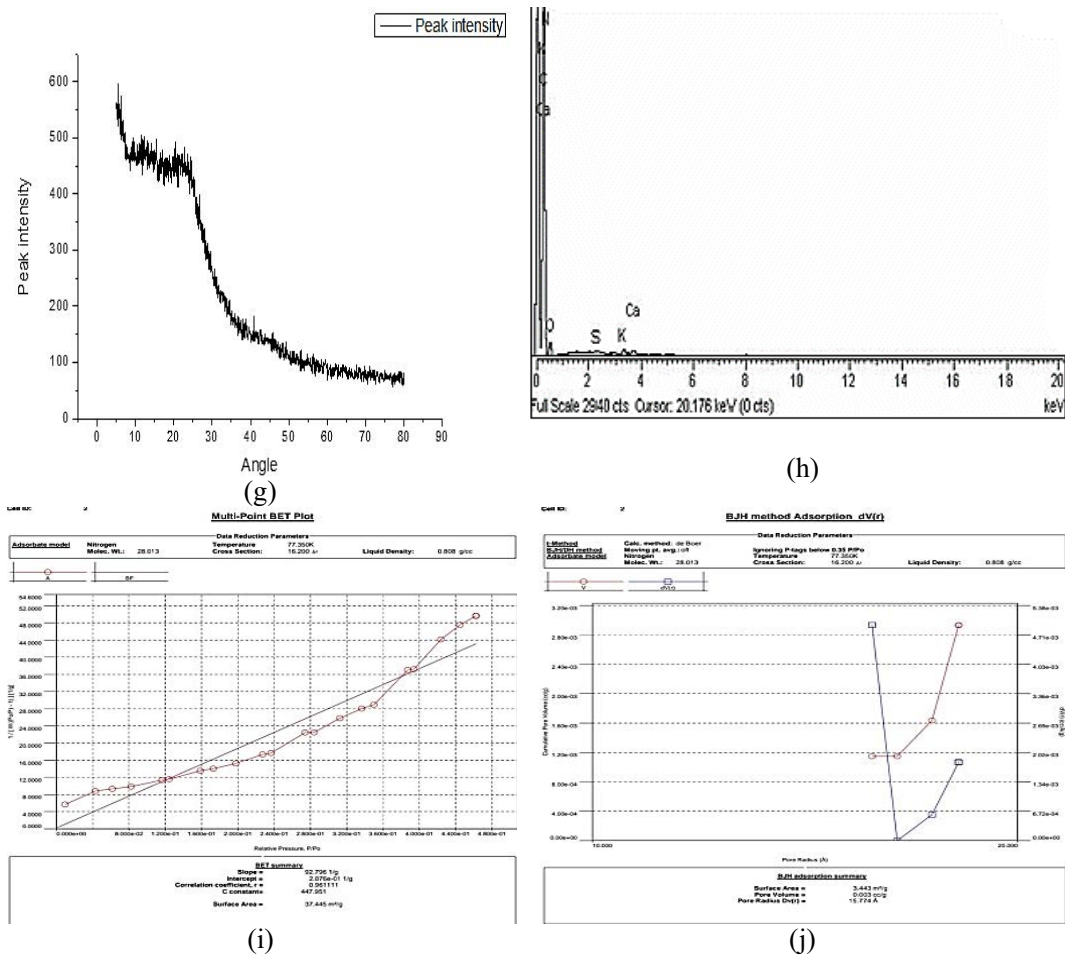


Fig. 2. Instrumental characterization of prepared AC. FTIR spectra of (a) AC, (b) Cd(II)-loaded AC, (c) Cr(VI)-loaded AC, (d) Pb(II)-loaded AC; SEM images of (e) AC, (f) TGA plot, (g) XRD plot, (h) EDX plot, (i) BET surface area, and (j) BJH pore distribution plot.

thermal degradation of cellulose material. The third mass loss was observed above 380°C, which was attributed to the formation of carbonaceous residues.

To identify the amorphous or crystalline nature of AC, XRD analysis was performed as shown in Fig. 2g. The pattern shown in the figure suggests the amorphous nature of the prepared adsorbent.

The elemental analysis (EDX) results have been presented in Fig. 2h. The carbon and oxygen are more prominent as compared with other small peaks of calcium, potassium, magnesium and sulphur that were present as impurities.

The BET surface area micrograph and BJH pore distribution plot are given in Figs. 2i and j. The BET, surface area, BJH pore volume, pore radius values were found to be 37.445 m² g⁻¹, 31.548 m² g⁻¹, 0.003 ccg⁻¹ and 3.443 Å, respectively.

3.2. Adsorption kinetics

The kinetics of Cd(II), Cr(VI) and Pb(II) adsorption on AC was investigated for fixed concentration solutions contacted with fixed amount of AC. The amount of metal adsorbed was plotted vs. time as shown in Fig. 3a. Initially,

the adsorption was fast as more adsorption sites were available; therefore, maximum adsorption took place in this step. Gradually the process slows down till the attainment of equilibrium as the active sites of AC were already occupied by metal ions.

The adsorption kinetics data were then fed into pseudo-first order, pseudo-second order, power function, Natarajan–Khalaf and intraparticle diffusion models to enumerate the adsorption kinetic parameters. The mathematical forms of these models are given as follows:

Pseudo-first order kinetic equation [28]:

$$\ln(q_e - q_t) = \ln q_e - K_1 t \tag{3}$$

Pseudo-second order kinetic equation [29]:

$$\frac{t}{q_t} = \frac{1}{K_2 q_e^2} + \frac{t}{q_e} \tag{4}$$

Power function kinetic model [30]:

$$\log q_t = \log a + b \log t \tag{5}$$

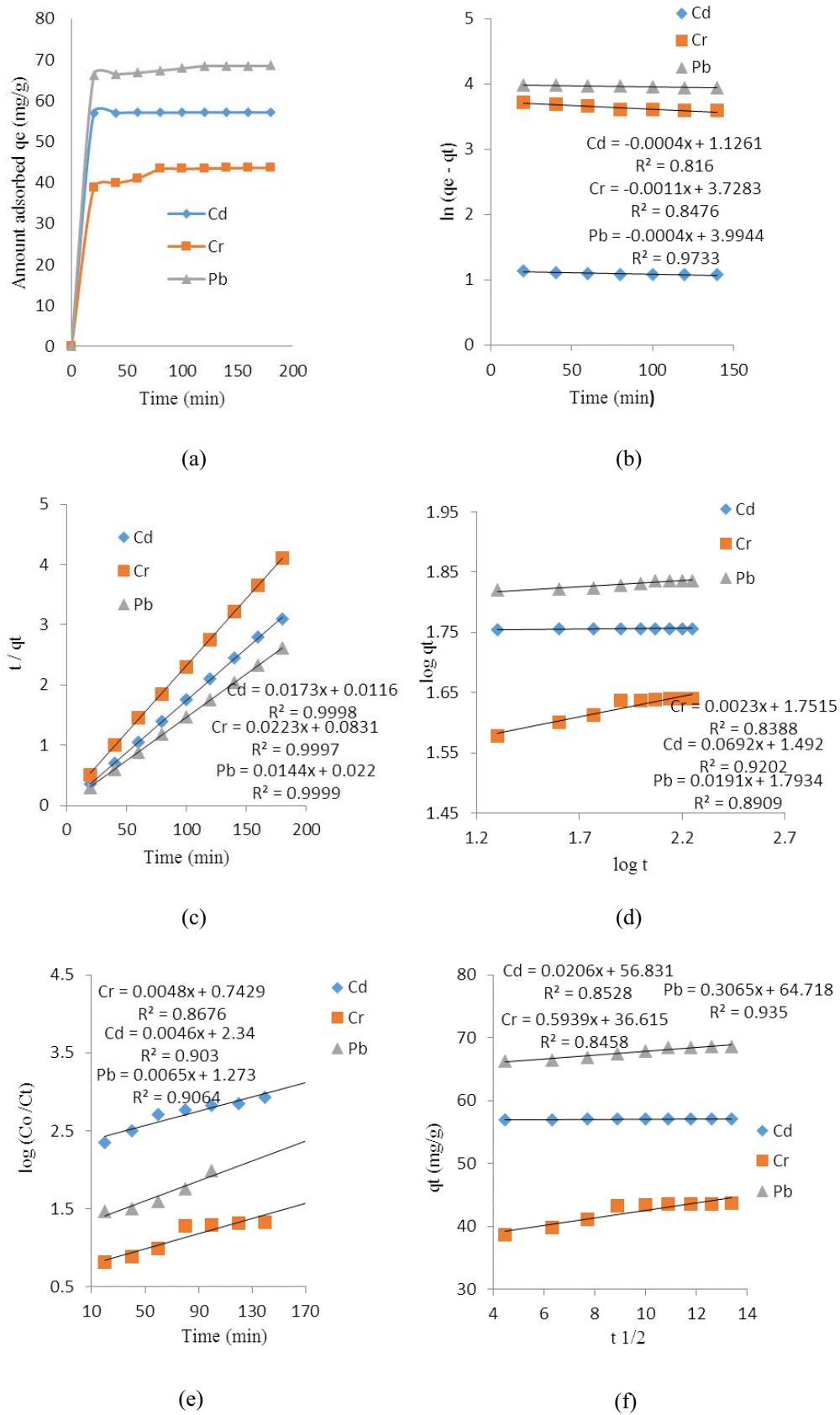


Fig. 3. Adsorption kinetics plots: (a) effect of contact time, (b) pseudo-first order kinetics model, (c) pseudo-second order kinetics model, (d) Power function kinetics model, (e) Natarajan and Khalaf kinetics model and (f) intraparticle diffusion model.

Natarajan and Khalaf kinetic equation [31]:

$$\log\left(\frac{C_0}{C_t}\right) = \frac{K_N}{2.303} t \quad (6)$$

Intraparticle diffusion equation [32,33]:

$$q_t = K_{\text{diff}} t^{1/2} + C \quad (7)$$

In Eq. (3), q_e (mg g^{-1}) is the amount of metal adsorbed at equilibrium while q_t at any time t , and K_1 (min^{-1}) is rate constant of first order equation. The value of K_1 and q_e was calculated from the slope and intercept of $\ln(q_e - q_t)$ vs. t plot as shown in Fig. 3b and are given in Table 1.

In Eq. (4), K_2 is pseudo-second order rate constant ($\text{g mg}^{-1} \text{min}$), q_e (mg g^{-1}) is the amount of metal adsorbed at equilibrium while q_t at any time t . The q_e and K_2 values were determined from intercept and slope of t/q_t vs. t plot as shown in Fig. 3c and are given in Table 1.

In Eq. (5), the constant a represents the initial rate of adsorption while constant b represents the reaction rate. Both these constants can be estimated from the intercept and slope of the $\log q_t$ vs. $\log t$ plot as shown in Fig. 3d. Their values are given in Table 1.

In Eq. (6), C_0 and C_t are concentrations at zero time and at time t , respectively. K is rate constant (min^{-1}), which can be calculated from slope of $\log(C_0/C_t)$ vs. t plot as shown in Fig. 3e and is given in Table 1.

In Eq. (7), q_t is the amount of metal adsorbed per unit mass of AC at any time t , K_{diff} ($\text{mg g}^{-1} \text{min}^{1/2}$) is the rate constant of intraparticle diffusion model and C (mg g^{-1}) is a constant whose value can be estimated from the intercept of q_t vs. $t^{1/2}$ plot (Fig. 3f) and related to the boundary layer thickness (Table 1). The intraparticle diffusion plot is obtained by plotting as shown in Fig. 3f. The linear portions of all the curves in Fig. 3f do not pass through the origin of

the graph that clearly shows that the intraparticle diffusion is not the only rate-controlling step in the adsorption process.

Based on R^2 value, it was concluded that adsorption of Cd(II), Cr(VI) and Pb(II) by AC follow well the pseudo-second order kinetic model.

3.3. Isotherm studies

A series of standard solutions of Cd(II), Cr(VI) and Pb(II) with concentrations of 20–200 mg L^{-1} were treated with AC and analysed after filtration using atomic absorption spectrophotometer. The effect of initial metal ions concentration is evident from Fig. 4a showing that the adsorption capability has been enhanced due to increase in concentration gradient, which may be due to opening of internal pores. With increase in heavy metal ion concentrations the transfer of mass between solution and AC has increased therefore, high adsorption was observed at high concentrations. Isothermal studies are significantly important while determining the adsorption capacities of adsorbent and give an idea about adsorbate and adsorbent interactions. Various isothermal models such as Freundlich, Langmuir, Temkin, Jovanovic and Harkins–Jura were applied to find out the isothermal parameters and explained the observed adsorption behaviour.

3.3.1. Freundlich adsorption isotherm

This model is used to explain the adsorption in monolayer with active sites having different energies [34]. The linear form of this model can be given as follows:

$$\ln q_e = \log K_f + \frac{1}{n} \ln C_e \quad (8)$$

where q_e is the adsorbate amount adsorbed per unit mass of AC (mg/g), C_e is adsorbate concentration in the solution

Table 1
Kinetic parameters of Cd(II), Cr(VI) and Pb(II) adsorption on AC

Kinetics model	Parameters	Metal ion		
		Cd(II)	Cr(VI)	Pb(II)
Pseudo-first order	K_1 (1/min)	4.0×10^{-4}	1.1×10^{-3}	4.0×10^{-4}
	q_e (mg/g)	3.083	41.60	54.29
	R^2	0.816	0.8476	0.9733
Pseudo-second order	K_2 (1/min)	2.58×10^{-2}	5.9×10^{-3}	9.4×10^{-3}
	q_e (mg/g)	57.80	44.84	69.44
	R^2	0.9998	0.9997	0.9999
Power function kinetics	α	56.42	31.04	62.14
	b	0.0023	0.0692	0.0191
	R^2	0.8388	0.9202	0.8909
Natarajan and Khalaf	K_N (1/min)	1.05×10^{-2}	1.1×10^{-2}	1.49×10^{-2}
	R^2	0.903	0.8676	0.9064
Intraparticle diffusion	K_{diff} ($\text{mg/g min}^{1/2}$)	0.0206	0.593	0.306
	C	56.83	36.61	64.71
	R^2	0.8528	0.8458	0.935

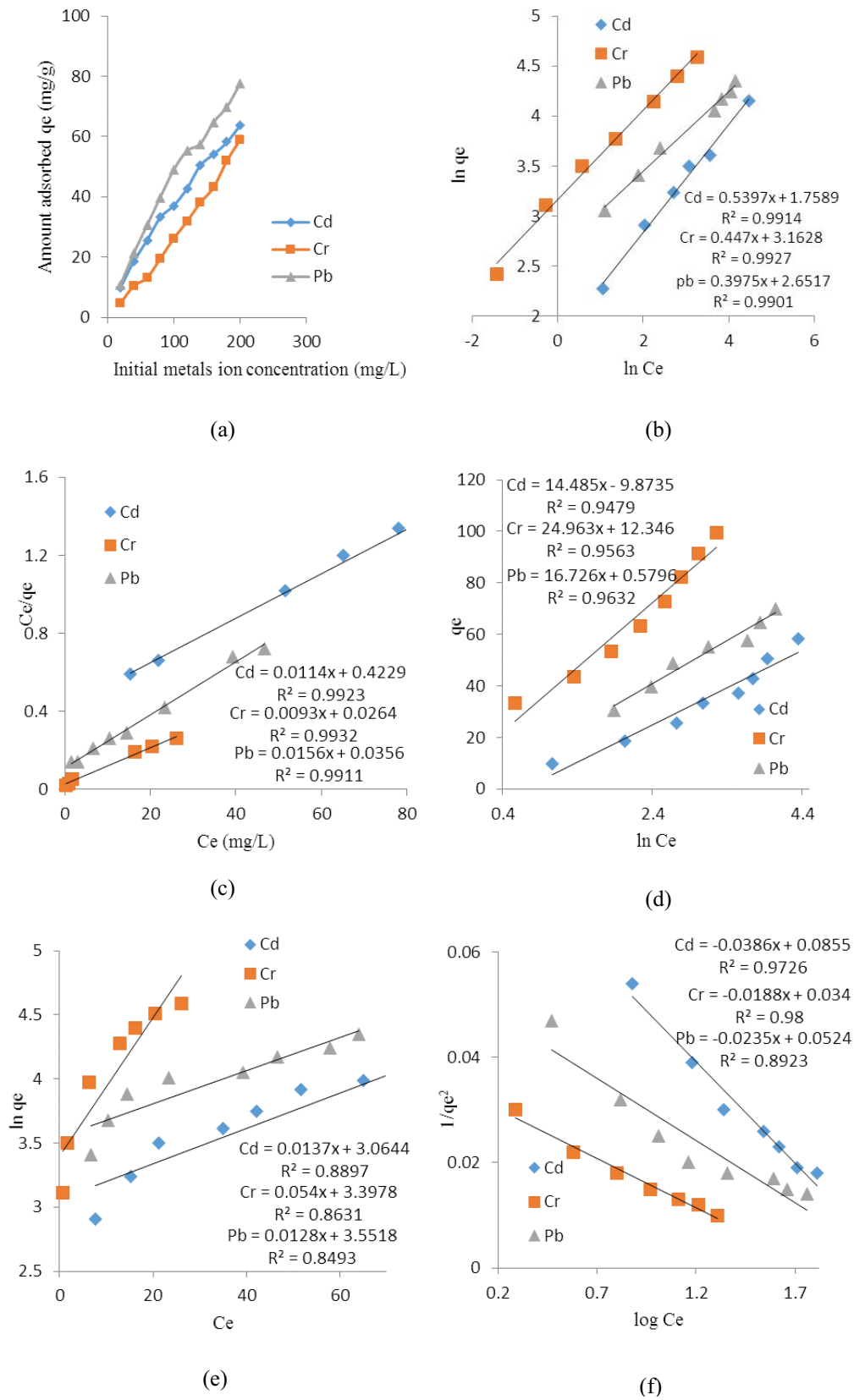


Fig. 4. Isotherm studies: (a) effect of initial metal ion concentration, (b) Freundlich plot, (c) Langmuir isotherm plot, (d) Temkin isotherm plot, (e) Jovanovic isotherm plot and (f) Harkins–Jura isotherm plot.

at equilibrium (mg L^{-1}), K_F is Freundlich constant and n is adsorption coefficient. K_F and n can be determined from slope and intercept of $\ln q_e$ vs. C_e plot as shown in Fig. 4b while their values are given in Table 2.

3.3.2. Langmuir adsorption isotherm

Linear form of this model can be given as follows [35]:

$$\frac{C_e}{q_e} = \frac{1}{K_L q_m} + \frac{C_e}{q_m} \quad (9)$$

where q_e is quantity of adsorbate adsorbed per unit mass of adsorbent at equilibrium, q_{max} is maximum adsorption capability, C_e is adsorbate concentration in solution at equilibrium and K_L is Langmuir constant (L mg^{-1}). From plot of C_e/q_e vs. C_e as shown in Fig. 4c, the values of q_{max} and K_L were obtained and are given in Table 2.

3.3.3. Temkin adsorption isotherm

The Temkin adsorption isotherm correlates the heat of adsorption with the surface coverage. The Temkin isotherm is valid only for an intermediate range of adsorbate concentrations [36,37]. The linear form of this isotherm is given as follows:

$$q_e = \beta \ln \alpha + \beta \ln C_e \quad (10)$$

where $\beta = RT/b$, R is a general gas constant and its value is 8.314 J/mol K , T is absolute temperature (K), β is a constant and related to the heat of adsorption. Plotting q_e against $\ln C_e$ a curve as shown in Fig. 4d was obtained and the estimated values of constant are given in Table 2.

3.3.4. Jovanovic adsorption isotherm

This model of adsorption was introduced by Jovanovic. The Jovanovic isotherm is nearly similar to Langmuir isotherm. However, it also considers the possibility of some mechanical interactions between adsorbate and adsorbent. The linear form of Jovanovic isotherm is given as follows [38]:

$$\ln q_e = \ln q_{\text{max}} - K_j C_e \quad (11)$$

where q_e represents the amount of adsorbate adsorbed per unit mass of adsorbent (mg g^{-1}), q_{max} is maximum adsorption capacity of adsorbent that can be obtained from the intercept of the graph, while C_e is equilibrium concentration (mg L^{-1}). The values of K_j and q_{max} were calculated from the slope and intercept of $\ln q_e$ vs. C_e plot as shown in Fig. 4e and their values are given in Table 2.

3.3.5. Harkins-Jura isotherm

Harkins-Jura isotherm considers multilayer adsorption possibility on the adsorbent surface having heterogeneous pore distribution [39]. The linear form of the Harkins-Jura isotherms can be given as follows:

$$\frac{1}{q_e^2} = \frac{B_H}{A_H} - \frac{1}{A_H} \log C_e \quad (12)$$

where B and A are Harkins-Jura constants (Table 2), which can be obtained from $1/q_e^2$ vs. $\log C_e$ plot as shown in Fig. 4f.

Based on R^2 value, it was concluded that Langmuir model can effectively accommodate the experimental data with high regression constant values.

Table 2
Isothermal parameters for adsorption of Cd(II), Cr(VI) and Pb(II) on AC

Isotherm models	Parameters	Metal ion		
		Cd(II)	Cr(VI)	Pb(II)
Freundlich	K_F (mg g^{-1})	5.806	23.63	14.17
	n	1.852	2.237	2.515
	R^2	0.9914	0.9927	0.9901
Langmuir	q_{max} (mg g^{-1})	81.71	107.5	64.10
	K_L (L mg^{-1})	0.0269	0.352	0.438
	R^2	0.9923	0.9932	0.9911
Temkin	β	14.48	24.96	16.72
	α	1.977	1.639	1.035
	b	156.69	90.92	135.70
	R^2	0.9479	0.9563	0.9632
Jovanovic	K_j (L g^{-1})	0.0137	0.054	0.0128
	q_{max} (mg g^{-1})	21.42	29.89	34.87
	R^2	0.8897	0.8631	0.8493
Harkins-Jura	A_H ($\text{g}^2 \text{L}^{-1}$)	25.90	53.19	42.55
	B_H ($\text{mg}^2 \text{L}^{-1}$)	2.215	1.808	2.229
	R^2	0.9726	0.98	0.8923

3.4. Effect of solution pH

The effect of solution pH on adsorption of Cd(II), Cr(VI) and Pb(II) is shown in Fig. 5. Initially the adsorption rate increases with increasing pH. Maximum adsorption of Cd(II) on AC occurred at pH 6 while for Cr(VI) and Pb(II) adsorption maxima was observed at pH 5 and 7, respectively. At low pH more H_3O^+ ions were there to compete with Cd(II), Cr(VI) and Pb(II) ions in getting adsorbed on to adsorbent surface [40]. Therefore, adsorption rate was low at acidic pH and that's why maximum adsorption has been recorded near neutral pH. Further increasing the pH resulted in no significant increase in the adsorption rate, which is due to ions saturation at the surface of AC, and remained constant in case of Cr while for Pb and Cd, a decline was observed at high pH.

3.5. Effect of adsorbent dosage

The effect of adsorbent dosage on Cd(II), Cr(VI) and Pb(II) adsorption was studied in the range of 0.01–0.1 g as shown in Fig. 6. It is clear from the graph that adsorption of Cd(II), Cr(VI) and Pb(II) increases with increase in the amount of AC. Significantly high adsorption was observed at 0.07 g dosage. Therefore 0.07 g of AC was taken as optimum dosage in all subsequent batch experiments.

3.6. Thermodynamic parameters

To determine the thermodynamic parameters, adsorption experiments were carried out at 298, 308, 318 and 328 K. From Van't Hoff plot, values of the parameters such as standard enthalpy change (ΔH°) and standard entropy change (ΔS°) were estimated [41]. The given plot is based on the following equation:

$$\ln K = \frac{\Delta S^\circ}{R} - \frac{\Delta H^\circ}{RT} \quad (13)$$

where $K = q_e/C_e$ and represents adsorption capacity, q_e (mg/g) is the adsorbate amount adsorbed at equilibrium, C_e is the concentration of adsorbate at equilibrium, R is the

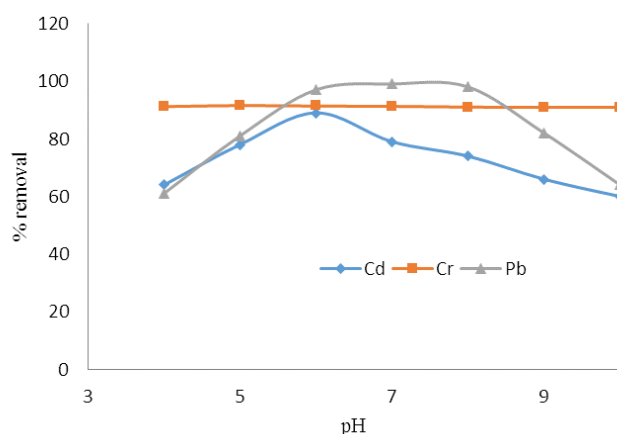


Fig. 5. Solution pH effect on adsorption.

universal gas constant, and T is temperature in Kelvin. ΔH° and ΔS° for Cd(II), Cr(VI) and Pb(II) were calculated from $\ln K$ against $1/T$ plot as shown in Fig. 7 and their values are given in Table 3. The negative values of ΔH° and positive values of ΔS° indicate exothermic and spontaneous nature of the process.

The Gibbs energy change (ΔG°) was calculated using the following equation [42].

$$\Delta G^\circ = \Delta H^\circ - T(\Delta S^\circ) \quad (14)$$

The negative values of ΔG° correspond to the favourable and spontaneous nature of the process.

3.7. Reusability of adsorbent

The reusability of the prepared sorbent was checked for five cycles. The percentage of adsorption decreased slightly from cycle to cycle as given in Fig. 8. This decrease is due to the destructive effect of the stripping agent and mass loss of the adsorbent during desorption treatment.

3.8. Comparison with other adsorbents

The *Populus nigra* sawdust-based activated carbon used in this study was compared with the reported activated carbons prepared from other biomass sources. Table 4 shows that the monolayer adsorption capacity of the prepared adsorbent is comparable with that of the other activated carbons reported in literature and thus could be used as an efficient adsorbent for the removal of heavy metals from water.

4. Conclusion

Adsorption is the most efficient environmental reclamation technique, which can remove minute amount of contaminant even at ppb level from aqueous solutions efficiently. In the present research work, an activated carbon was prepared from sawdust of *Populus nigra*. The synthesized AC was characterized by FTIR, SEM, TGA, EDX, XRD and surface area analysis. The prepared adsorbent quite efficiently removed Cd(II), Cr(VI) and Pb(II) from test

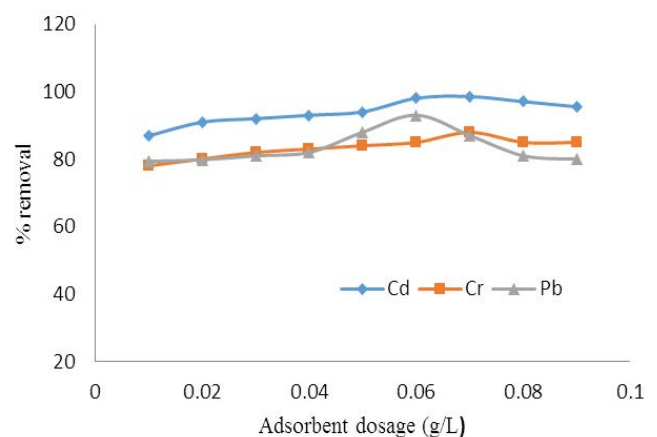


Fig. 6. Effect of adsorbent dosage.

Table 3
Thermodynamic parameters of Cd(II), Cr(VI) and Pb(II) adsorption on AC

Metal ion	ΔH° (kJ/mol)	ΔS° (kJ/mol)	ΔG° (kJ/mol)			
			298 K	308 K	318 K	328 K
Cd(II)	-46.64	164.06	-48.93	-50.74	-52.21	-53.85
Cr(VI)	-4.32	28.87	-8.60	-8.89	-9.18	-9.43
Pb(II)	-46.14	187.27	-55.85	-57.91	-59.59	-61.47

Table 4
Comparison with other activated carbon

Adsorbents	q_{\max} (mg/g)			References
	Cd(II)	Cr(VI)	Pb(II)	
Water hyacinth (<i>Eichhornia crassipes</i>) plant activated carbon	37.78			[42]
Marine green algae activated carbon	22.93			[43]
<i>Cicer arietinum</i> activated carbon	20.69			[44]
<i>Eichhornia crassipes</i> activated carbon	16.61			[45]
This study	81.71			
<i>Leucaena leucocephala</i> activated carbon		70.42		[46]
<i>Mauritia flexuosa</i> activated carbon		26.33		[47]
<i>Cicer arietinum</i> activated carbon		17.77		[44]
Olive stone activated carbon		11.72		[48]
This study		107.5		
Rubber wood sawdust activated carbon			44.05	[49]
<i>Pinus roxburghii</i> activated carbon			29.58	[50]
Almond shell activated carbon			19.98	[51]
Coconut shell activated carbon			10.88	[52]
This study			64.10	

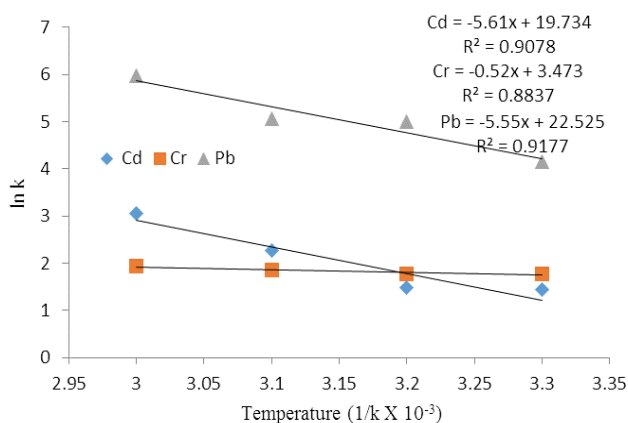


Fig. 7. Van't Hoff plot for Cd(II), Cr(VI) and Pb(II) adsorption on AC.

solutions. At the maximum adsorption, the optimum pH occurred was 6, 5 and 7, respectively, for Cd(II), Cr(VI) and Pb(II). The Langmuir isotherm and pseudo-second order kinetic model well fitted the equilibrium and kinetics data with high R^2 values. From the calculated thermodynamic

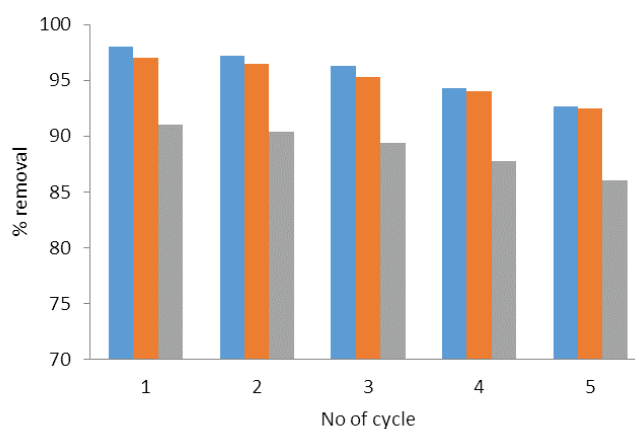


Fig. 8. Reusability of the prepared activated carbon.

parameters such as ΔH° , ΔS° and ΔG° , it was inferred that the adsorption of Cd(II), Cr(VI) and Pb(II) by AC was favourable, spontaneous and exothermic in nature. From the results, it was concluded that the prepared AC could be used as low-cost adsorbent for the removal of Cd(II), Cr(VI) and Pb(II) ions from aqueous media.

Data availability statement

All the data associated with this research have been presented in this paper.

References

- [1] R. Apiratikul, P. Pavasant, Batch and column studies of biosorption of heavy metals by *Caulerpa lentillifera*, *Bioresour. Technol.*, 99 (2008) 2766–2777.
- [2] H. Chen, J. Zhao, G. Dai, J. Wu, H. Yan, Adsorption characteristics of Pb(II) from aqueous solution onto a natural biosorbent, fallen *Cinnamomum camphora* leaves, *Desalination*, 262 (2010) 174–182.
- [3] H. Marsh, F.R. Reinoso, *Activated Carbon*, Elsevier Science, North Shields, UK, 2006, pp. 13–86.
- [4] J. Wang, C. Chen, Biosorbents for heavy metals removal and their future, *Biotechnol. Adv.*, 27 (2009) 195–226.
- [5] M. Kasuya, H. Teranishi, K. Aoshima, T. Katoh, H. Horiguchi, Y. Morikawa, K. Iwata, Water pollution by cadmium and the onset of Itai-itai disease, *Water Sci. Technol.*, 25 (1992) 149–156.
- [6] M. Yasuda, A. Miwa, M. Kitagawa, Morphometric studies of renal lesions in itai-itai disease: chronic cadmium nephropathy, *Nephron*, 69 (1995) 14–19.
- [7] K. Kadirvelu, K. Thamaraiselvi, C. Namasivayam, Removal of heavy metals from industrial wastewaters by adsorption onto activated carbon prepared from an agricultural solid waste, *Bioresour. Technol.*, 76 (2001) 63–65.
- [8] M. Mohapatra, S. Anand, Studies on sorption of Cd(II) on Tata chromite mine overburden, *J. Hazard. Mater.*, 148 (2007) 553–559.
- [9] J.M. Chen, O.J. Hao, Microbial chromium(VI) reduction, *Crit. Rev. Environ. Sci. Technol.*, 28 (1998) 219–251.
- [10] A. Papandreou, C. Stournaras, D. Papias, Copper and cadmium adsorption on pellets made from fired coal fly ash, *J. Hazard. Mater.*, 148 (2007) 538–547.
- [11] G. Dermont, M. Bergeron, G. Mercier, M. Richer-Lafleche, *Metal-Contaminated Soils: Remediation Practices and Treatment Technologies*, *Pract. Period. Hazard. Toxic Radioact. Waste Manage.*, 12 (2008) 188–209.
- [12] N. Dizge, B. Keskinler, H. Barlas, Sorption of Ni(II) ions from aqueous solution by Lewatit cation-exchange resin, *J. Hazard. Mater.*, 167 (2009) 915–926.
- [13] O. Hamdaoui, Removal of copper(II) from aqueous phase by Purolite C100-MB cation exchange resin in fixed bed columns: modeling, *J. Hazard. Mater.*, 161 (2009) 737–746.
- [14] H.Y. Shim, K.S. Lee, D.S. Lee, D.S. Jeon, M.S. Park, J.S. Shin, D.Y. Chung, Application of electrocoagulation and electrolysis on the precipitation of heavy metals and particulate solids in washwater from the soil washing, *J. Agric. Chem. Environ.*, 3 (2014) 130.
- [15] J.C. Crittenden, K. Li, D. Minakata, P. Westerhoff, H. Jeong, D. Hokanson, R. Trussell, Understanding and Improving Process Performance of Advanced Oxidation Processes (AOPs), *The Croucher Foundation Advanced Study Institute (ASI)*, Hong Kong, China, June 23–27, 2008.
- [16] Y. Ku, I.L. Jung, Photocatalytic reduction of Cr(VI) in aqueous solutions by UV irradiation with the presence of titanium dioxide, *Water Res.*, 35 (2001) 135–142.
- [17] S. Muthusarayanan, N. Sivarajasekar, J.S. Vivek, T. Paramasivan, M. Naushad, J. Prakashmaran, V. Gayathri, O.K. Al-Duaij, Phytoremediation of heavy metals: mechanisms, methods and enhancements, *Environ. Chem. Lett.*, 16 (2018) 1339–1359.
- [18] G.Z. Kyzas, G. Bomis, R.I. Kosheleva, E.K. Efthimiadou, E.P. Favvas, M. Kostoglou, A.C. Mitropoulos, Nanobubbles effect on heavy metal ions adsorption by activated carbon, *Chem. Eng. J.*, 356 (2019) 91–97.
- [19] I. Ali, New generation adsorbents for water treatment, *Chem. Rev.*, 112 (2012) 5073–5091.
- [20] S. Lata, P.K. Singh, S.R. Samadder, Regeneration of adsorbents and recovery of heavy metals: a review, *Int. J. Environ. Sci. Technol.*, 12 (2015) 1461–1478.
- [21] R.K. Gautam, A. Mudhoo, G. Lofrano, M.G. Chattopadhyaya, Biomass-derived biosorbents for metal ions sequestration: adsorbent modification and activation methods and adsorbent regeneration, *J. Environ. Chem. Eng.*, 2 (2014) 239–259.
- [22] D. Tang, Z. Zheng, K. Lin, J. Luan, J. Zhang, Adsorption of p-nitrophenol from aqueous solutions onto activated carbon fiber, *J. Hazard. Mater.*, 143 (2007) 49–56.
- [23] M. Wahab, M. Zahoor, S.M. Salman, A novel approach to remove ofloxacin antibiotic from industrial effluent using magnetic carbon nanocomposite prepared from sawdust of *Dalbergia sissoo* by batch and membrane hybrid technology, *Desal. Water Treat.*, 165 (2019) 83–96.
- [24] C. Obi, O.E. Njoku, Removal of Ni(II) and Pb(II) ions from aqueous solutions by grapefruit (*Citrus paradisi*) mesocarp biomass, *J. Appl. Sci. Environ. Manage.*, 19 (2015) 536–444.
- [25] E. Jayamani, S. Hamdan, M.R. Rahman, M.K.B. Bakri, Study of sound absorption coefficients and characterization of rice straw stem fibers reinforced polypropylene composites, *Bioresour. Technol.*, 10 (2015) 3378–3392.
- [26] M.D. Mashitah, Zur/odhly, S. Bhatla, Binding mechanism of heavy metals biosorption by *Pycnoporus Sanguineus*, *Artif. Cells Blood Substitutes Biotechnol.*, 27 (1999) 441–445.
- [27] D. Liu, K. Xia, R. Yang, J. Li, K. Chen, M. Nazhad, Manufacturing of a biocomposite with both thermal and acoustic properties, *J. Compos. Mater.*, 46 (2012) 1011–1020.
- [28] S. Lagergren, B. Svenska, On the theory of so-called adsorption of materials, *R. Swed. Acad. Sci. Doc.*, 24 (1898) 1–13.
- [29] Y. Ho, J. Ng, G. McKay, Kinetics of pollutant sorption by biosorbents, *Sep. Purif. Technol.*, 29 (2000) 189–232.
- [30] K. Riahi, S. Chaabane, B.B. Thayer, A kinetic modeling study of phosphate adsorption onto *Phoenix dactylifera* L. date palm fibers in batch mode, *J. Saudi Chem. Soc.*, 21 (2017) 143–152.
- [31] W. Cheung, J. Ng, G. McKay, Kinetic analysis of the sorption of copper(II) ions on chitosan, *J. Chem. Technol. Biotechnol.*, 78 (2003) 562–571.
- [32] S. Srivastava, R. Tyagi, N. Pant, Adsorption of heavy metal ions on carbonaceous material developed from the waste slurry generated in local fertilizer plants, *Water Res.*, 23 (1989) 1161–1165.
- [33] W.J. Weber, J.C. Morris, Kinetics of adsorption on carbon from solution, *J. Agric. Eng. Res.*, 89 (1963) 31–60.
- [34] H. Freundlich, Über die adsorption in losungen “Adsorption in solution”, *Z. Phys. Chem.*, 57 (1906) 385–470.
- [35] I. Langmuir, The constitution and fundamental properties of solids and liquids. Part I. Solids, *J. Am. Chem. Soc.*, 38 (1916) 2221–2295.
- [36] H. Shahbeig, N. Bagheri, S.A. Ghorbanian, A. Hallajisani, S. Poorkarimi, A new adsorption isotherm model of aqueous solutions on granular activated carbon, *Int. Simul. Model.*, 9 (2013) 243–254.
- [37] M. Samarghandi, M. Hadi, S. Moayedi, A.F. Barjesteh, Two-parameter isotherms of methyl orange sorption by pinecone derived activated carbon, *Iran. J. Environ. Health Sci. Eng.*, 6 (2009) 285–294.
- [38] N. Ayawei, A.N. Ebelegi, D. Wankasi, Modelling and interpretation of adsorption isotherms, *J. Chem.*, 2017 (2017) 1–11.
- [39] K.Y. Foo, B.H. Hameed, Insights into the modelling of adsorption isotherm systems, *Chem. Eng. J.*, 156 (2010) 2–10.
- [40] F. Hernáinz, M. Calero, G. Blázquez, M. Martín-Lara, G. Tenorio, Comparative study of the biosorption of cadmium(II), chromium(III), and lead(II) by olive stone, *Environ. Prog. Sustain.*, 27 (2008) 469–478.
- [41] Q. Falcoz, D. Gauthier, S.P. Abanades, G. Flamant, F. Patisson, Kinetic rate laws of Cd, Pb, and Zn vaporization during municipal solid waste incineration, *Environ. Sci. Technol.*, 43 (2009) 2184–2189.
- [42] S. Qiu, L. Wu, X. Pan, L. Zhang, H. Chen, C. Gao, Preparation and properties of functionalized carbon nanotube/PSF blend ultrafiltration membranes, *J. Membr. Sci.*, 342 (2009) 165–172.
- [43] A. El-Wakil, W. Abou El-Maaty, F. Awad, Removal of lead from aqueous solution on activated carbon and modified activated

- carbon prepared from dried water hyacinth plant, *J. Anal. Bioanal. Tech.*, 5 (2014) 1–14.
- [44] R.S. Jeyakumar, V. Chandrasekaran, Adsorption of lead(II) ions by activated carbons prepared from marine green algae: equilibrium and kinetics studies, *Int. J. Ind. Chem.*, 5 (2014) 2.
- [45] D. Ramana, K. Jamuna, B. Satyanarayana, B. Venkateswarlu, M.M. Rao, K. Seshiah, Removal of heavy metals from aqueous solutions using activated carbon prepared from *Cicer arietinum*, *Environ. Toxicol. Chem.*, 92 (2010) 1447–1460.
- [46] C. Gérente, P.C. Du Mesnil, Y. Andrès, J.F. Thibault, P. Le Cloirec, Removal of metal ions from aqueous solution on low cost natural polysaccharides: sorption mechanism approach, *React. Funct. Polym.*, 46 (2000) 135–144.
- [47] W.M.H. Wan Ibrahim, M.H. Mohamad Amini, N.S. Sulaiman, W.R.A. Kadir, Powdered activated carbon prepared from *Leucaena leucocephala* biomass for cadmium removal in water purification process, *Arab. J. Basic Appl. Sci.*, 26 (2019) 30–40.
- [48] D. Obregón-Valencia, M. del Rosario Sun-Kou, Comparative cadmium adsorption study on activated carbon prepared from aguaje (*Mauritia flexuosa*) and olive fruit stones (*Olea europaea* L), *J. Environ. Chem. Eng.*, 2 (2014) 2280–2288.
- [49] T.M. Alslaibi, I. Abustan, M.A. Ahmad, A.A. Foul, Cadmium removal from aqueous solution using microwaved olive stone activated carbon, *J. Environ. Chem. Eng.*, 1 (2013) 589–599.
- [50] T. Karthikeyan, S. Rajgopal, L.R. Miranda, Chromium(VI) adsorption from aqueous solution by *Hevea Brasilinesis* sawdust activated carbon, *J. Hazard. Mater.*, 124 (2005) 192–199.
- [51] M.J. Saif, K.M. Zia, F. Ur-Rehman, M. Usman, A.I. Hussain, S.A.S. Chatha, Removal of heavy metals by adsorption onto activated carbon derived from pine cones of *Pinus roxburghii*, *Water Environ. Res.*, 87 (2015) 291–297.
- [52] E. Demirbas, M. Koby, E. Senturk, T. Ozkan, Adsorption kinetics for the removal of chromium(VI) from aqueous solutions on the activated carbons prepared from agricultural wastes, *Water SA*, 30 (2004) 533–539.